Eur. Phys. J. D **38**, 163–173 (2006)
DOI: 10.1140/epjd/e2006-00014-6

THE EUROPEAN PHYSICAL JOURNAL D

Dissociation mechanism of electronically excited CH_n (n = 3–5) neutrals formed by near-resonant neutralization using charge inversion mass spectrometry

S. Hayakawa[a] and N. Kabuki

Department of Chemistry, Graduate School of Science, Osaka Prefecture University, 1-1 Gakuen-cho, Sakai, Osaka 599-8531, Japan

Received 13 August 2005 / Received in final form 31 October 2005
Published online 17 January 2006 –

Abstract. Charge inversion mass spectrometry was used to produce the electronically excited species CH_n (n = 3–5) from their corresponding positive ions by neutralization with an alkali metal target, and then to subsequently detect and mass-analyze the negative ions formed from the neutral fragments produced from the dissociation of the excited neutrals. The trapezoidal shape and the intensity of the peak associated with CH_2^- ions in the charge inversion spectrum of CH_3^+ ions indicated that the CH_3 neutrals dissociated mainly into CH_2 + H without a large activation barrier. The most intense peak in the spectrum of CH_4^+ ions was that associated with CH_2^- ions, and this peak comprised a combination of both trapezoidal and triangular shaped peaks. The trapezoidal shaped peak was attributed to CH_2^- ions resulting from direct dissociation of CH_4 into CH_2 + H_2. The concurrent dissociation of CH_4 into CH_3 + H was followed by the further subsequent dissociation of the deformed CH_3 fragments into CH_2 + H, and this was proposed to be the origin of the triangular shaped component of the CH_2^- peak. In the spectrum of CH_5^+ ions, the CH_3^- peak was much less intense than the CH_2^- peak, which was proposed to be the result of the geometry of the CH_3, formed from the dissociation of CH_5 into CH_3 + H_2,being substantially distorted from the D_{3h} symmetry, leading to its further subsequent dissociation.

PACS. 34.50.Gb Electronic excitation and ionization of molecules; intermediate molecular states (including lifetimes, state mixing, etc.) – 34.70.+e Charge transfer – 34.50.Lf Chemical reactions, energy disposal, and angular distribution, as studied by atomic and molecular beams

1 Introduction

Excited neutral species, such as radicals, play an important role as intermediates in many chemical reactions, and the study of dissociation of these intermediates is indispensable for building fundamental knowledge about the dynamics of these chemical reactions. Moreover, the understanding of the dissociation mechanism of neutral species is relevant to a wide range of basic and applied sciences, including; molecular physics, quantum electronics, plasma discharge, quantum theory, atmospheric science, space science, environmental science and materials science.

The generation of isolated neutral intermediates in the gas phase is non-trivial due to their high reactivity, and the energy selection of these intermediates is even more difficult. We have discovered that excited unstable neutral species can be produced from the corresponding positive ions by single electron transfer using our charge inversion mass spectrometer, where the positive ions are then made to collide with alkali metal targets and the resulting negative ions formed upon two-electron transfer are mass-analyzed [1,2]. By using thermometer molecules, whose term is used to indicate that the internal energy distribution in the nascent electron transfer product can be estimated by a simple measurement of the masses and abundances of the fragment ions [3,4], we demonstrated that the process of dissociative negative ion formation in the charge inversion mass spectrometer occurs by near-resonant neutralization, followed by spontaneous dissociation of the neutrals, and then endothermic negative ion formation according to the following scheme [1,5,6];

$$\begin{aligned} AB^+ + T &\rightarrow AB^* + T^+ \\ AB^* &\rightarrow A + B \\ B + T &\rightarrow B^- + T^+. \end{aligned}$$

Unstable neutral intermediates, such as vinylidene, have been studied using this technique [7,8]. In the present work, the dissociation of CH_3, CH_4, and CH_5 formed from the corresponding positive ions are investigated using charge inversion mass spectrometry.

[a] e-mail: hayakawa@c.s.osakafu-u.ac.jp

The methyl free-radical (CH_3) is a primary intermediate in flames, plasmas, and photolytic reactions, and is also observed in planetary atmospheres and interstellar clouds, so an understanding of the unimolecular dissociation dynamics of CH_3 is important for these scientific fields. Since the pioneering measurements of the methyl radical using ultraviolet spectroscopy by Herzberg and coworkers [9,10], the photo-dissociation dynamics of the CH_3 radical have been investigated using a wide range of techniques, including; flash photolysis absorption [11], multiphoton ionization [12,13], rotational resonance Raman spectroscopy [14], photo-fragment translational spectroscopy [15], coherent infrared-ultraviolet double-resonance spectroscopy [16], and H-atom Rydberg tagging time-of-flight method with a pure CH_3 radical source [17]. The transition observed at 216 nm was assigned to the ($000 \leftarrow 000$) band of the electronic transition from the unpaired $2p_z$ electron to a $3s$ Rydberg orbital [10,11]. The pre-dissociation lifetime of the excited (000) level was determined to be less than 100 fs [14]. This rapid pre-dissociation of the $3s$ state of the CH_3 radical, which provided broad ultraviolet absorption, was attributed to cleavage of a C–H bond. Orbital correlations in the dissociation of the CH_3 radical were reported by Yu et al. [18] and indicated that the $3s$ Rydberg state ($\tilde{B}\ ^2A_1'$) was correlated to the singlet methylene, CH_2 ($\tilde{a}\ ^1A_1$), with a small barrier, and the ground-state CH_3 radical was correlated to two asymptotic dissociation channels, $CH_2(\tilde{X}\ ^3B_1)$ + H (^2S) and CH ($\tilde{X}\ ^2\Pi$) + H_2 ($^1\Sigma_g^+$). On the other hand, the reaction between CH and H_2 and their deuterated analogs was investigated as a function of both temperature and pressure by Lin and coworkers [19,20]. From the comparison of the Arrhenius plots and the transition state theory (RRKM) calculations of the reaction between CH and H_2, it was believed that the reaction of CH + H_2 had no activation energy. A crossed-beam study of the state-resolved dynamics of CH ($X^2\Pi$) + D_2 and its isotopic analog, namely, CD ($X^2\Pi$) + H_2, by Liu and coworkers indicated that reaction of CH + H_2 proceeded by a complex formation mechanism and had little or no activation energy [21,22]. Theoretical ab initio calculations also predicted that there was probably no barrier for the reaction to proceed with CH and H_2 approaching each other along the minimum energy path [23–25].

Knowledge about the dissociation pathway of methane (CH_4) molecules is of fundamental importance to organic chemistry. Dissociation of methane is also of atmospheric interest as methane is relatively abundant in the upper atmosphere of the earth and of other planets [26–28]. It is believed that the photo-dissociation of CH_4 in the atmosphere of the earth and other planets is driven primarily by intense solar atomic emission lines, such as Lyman–α radiation, and is one of the primary steps in the synthesis of higher hydrocarbons and other organic molecules.

The absorption spectrum of methane starts at approximately $\lambda < 145.5$ nm [29], and the absorption cross-section increases continuously towards shorter wavelengths, showing only minor fine-structure in the region between 145 nm and 100 nm [30–32]. The photo-absorption cross-section and fluorescence yield were measured using synchrotron radiation at 106.0–142.0 nm by Lee and Chiang [31]. Electron impact excitation was also investigated using a trapped-electron spectrometer by Curtis and Walker [33]. The photo-dissociation dynamics of CH_4, especially by Lyman–α, have been investigated using various methods, such as resonance fluorescence of ^2P–^2S line of hydrogen [34], H-atom photo-fragment translational spectroscopy [35], a photo-fragment imaging technique [36], Doppler-selected time-of-flight technique [37], and measurement of CH_2 and CH_3 abundances [38]. Theoretical calculations have also been performed using various calculation techniques [39–43]. The lowest $^1T_2$ state, which can be accessed at Lyman–α, correlates adiabatically with $CH_2(^1B_1)$ + H_2 product [39–43]. Due to this correlation, it was believed that CH_2 + H_2 were the major products of CH_4 photo-dissociation at Lyman–α. However, in 1993, Mordaunt and co-workers found, using the technique of H-atom photo-fragment translational spectroscopy, that simple C–H bond fission to form the CH_3 radical was the dominant primary process following Lyman–α absorption [35]. The resulting CH_3 fragments, which were formed with a very high level of internal excitation, underwent subsequent unimolecular decay, predominantly to CH + H_2. Heck et al. concluded that numerous different pathways contribute to the photo-dissociation mechanism [36]. Liu and coworkers differentiated three distinct pathways for C–H bond fission of CH_4 by Lyman–α absorption from the combined measurements for the photofragment kinetic energy release and the anisotropy parameter in the Doppler-selected time-of-flight technique in the photolysis of CH_4 and its isotopomers [37]. In their subsequent work, the relative abundances of methyl and methylene fragments formed from CH_4 and its isotopomers by Lyman–α absorption were measured by Lyman–α photoionization [38]. By combining both data, a complete set of quantum yields for the different photodissociation channels of CH_3 + H, CH_2 + H_2, CH_2 + 2H, and CH + H_2 + H, were reported for each isotopomers [38].

The dissociation of the transient CH_5 neutral has not previously been investigated because of the difficulty in producing CH_5 by conventional methods. Consequently, only investigations of CH_5^+ ions have been conducted to date. CH_5^+ ion is a well-known gas-phase reagent for chemical ionization mass spectrometry [44,45]. In fact, the process of CH_5^+ ion formation is described as $CH_4^+ + CH_4 = CH_5^+ + CH_3$, which was the first ion-molecule reaction observed in mass spectrometers using a high-pressure ion source [46]. Several theoretical calculations have been performed to determine the structures and potential surfaces of CH_5^+ ions [47–54]. Many earlier theoretical studies on CH_5^+ ion have reported various structures for CH_5^+ ions, and all concluded that the global minimum of CH_5^+ ions has C_s symmetry, with an H_2 molecule bound at the apex of a pyramidal CH_3^+ unit by a three-center two-electron bond [47–54]. Hiraoka and co-workers investigated experimentally the structure of CH_5^+ ions from the thermochemical stabilities of the

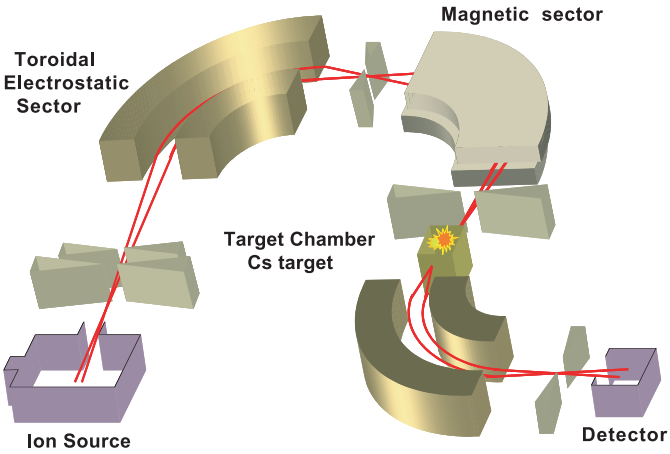

Fig. 1. The MS/MS instrument used for charge inversion mass spectrometry using alkali metal targets.

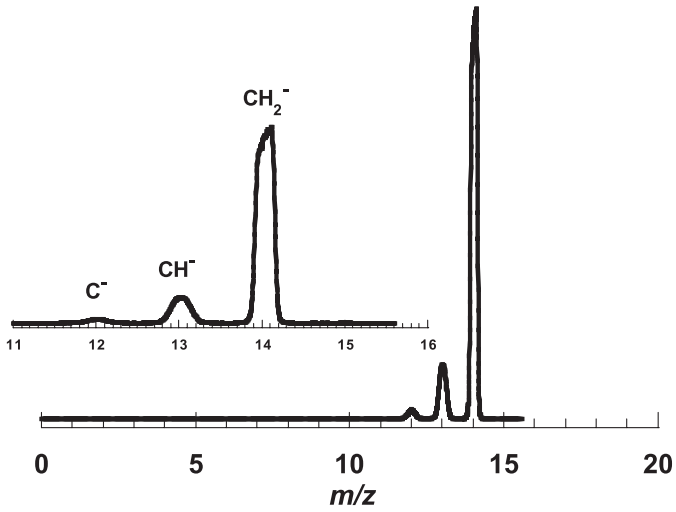

Fig. 2. The charge inversion spectrum of CH_3^+ on collision with a Cs target. The expanded spectrum of $m/z = 12$∼14 is shown in the inset.

cluster ions $CH_5^+(H_2)_n$ by measuring the temperature dependence of the equilibrium constant $CH_5^+(H_2)_{n-1} + 2H_2 = CH_5^+(H_2)_n + H_2$ [55].

In the present work, we compare the method of photo-excitation with that of neutralization from the corresponding cation, for studying the dissociation mechanism of CH_n ($n = 3$–5) neutrals. The formation and selection of the CH_n^+ ($n = 3$–5) species are straightforward for mass spectrometry. Detection of the neutral fragments was accomplished by converting the neutrals into negative ions by additional collisions with alkali metal targets. While most of photo-dissociation experiments detect the H atom or the H_2 molecule, except for the work by Lee and coworkers [15] and by Liu and coworkers [38], our charge inversion experiment can also detect heavier fragments, such as CH_n ($n = 0$–3). It is demonstrated in the present work that detection and analysis of these heavier dissociation fragments of the electronically excited neutrals formed from the corresponding cations in the charge inversion mass spectrometer provides useful complementary information to the technique of photo-dissociation.

2 Experimental

Charge inversion mass spectrometry was performed using an MS/MS instrument in which mass-separated positive ions are made to collide with alkali metal targets, and the resulting negative ions formed upon two successive single-electron transfers are mass analyzed [1,56]. The MS/MS instruments utilizes an Hitachi M80B double focusing mass spectrometer as MS-I to mass-separate precursor ions, and a toroidal electrostatic analyzer (ESA) as MS-II to mass-analyze secondary ions, as shown in Figure 1. Methane gas (Takachiho, Japan) was used as received, and was introduced into the ion source through a guide pipe. The positive ions were formed under electron ionization (EI) or chemical ionization (CI) conditions. CH_n^+ ($n = 3$–5) ions formed in the ion source were accelerated to 3 keV kinetic energy, and the precursor ions are mass separated by MS-I. The mass separated precursor ions CH_n^+ ($n = 3$–5) enter a 3.7 cm long target chamber which is located between the two analyzers. The alkali metal is introduced into the target chamber as a vapor from a reservoir through a ball valve. The target gas density in the target chamber is controlled with the ball valve and output power of the heaters. Neutralization, spontaneous dissociation and anionization take place in the target chamber filled with the alkali metal target (Cs). The negative ions are mass-analyzed by MS-II and detected by a 10 kV post-acceleration secondary electron multiplier.

3 Results and discussion

3.1 Dissociation of CH_3

The charge inversion spectrum of CH_3^+ ions measured using a Cs target is shown in Figure 2. The dominant peak is that associated with CH_2^- ions observed at $m/z = 14$, whereas the non-dissociative peak associated with CH_3^- ($m/z = 15$) is absent. In our previous studies on the charge inversion spectra using $C_2H_n^+$ ($n = 0$–2) ions obtained from acetylene, the sharp peaks observed at $m/z = 24$ and at $m/z = 25$ only for Cs target were assigned to non-dissociative C_2^- and the C_2H^- ions from C_2^+ and C_2H^+ ions, respectively [57,58]. The peaks associated with the non-dissociative C_2^- and C_2H^- ions showed the linear dependence on the density of the Cs target. Based on these results, it was confirmed that the non-dissociative C_2^- and C_2H^- ions were formed by double electron transfer in a single collision. If double electron transfer in a single collision is dominant in the present charge inversion mass spectrometer, then CH_3^- ions would be observed as a sharp peak associated with a non-dissociative process, analogously to the charge inversion spectra of C_2^+ and C_2H^+ ions. The absence of a sharp peak associated

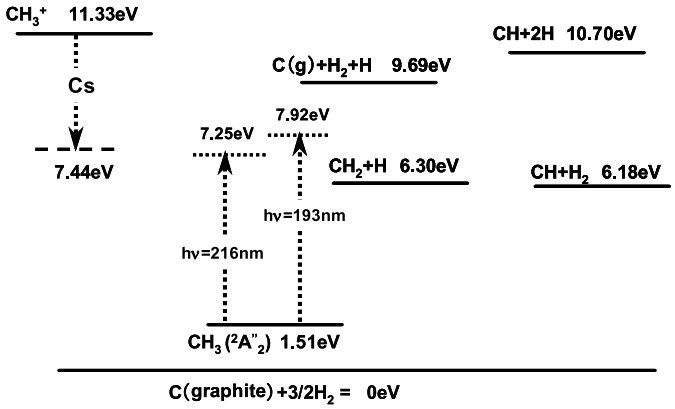

Fig. 3. The heats of formation of the neutral and cationic forms of CH_3. The thermochemical values are taken from reference [61]. The energy levels predicted by near-resonant neutralization with a Cs target and photo-excitation are shown as dashed and dotted lines, respectively.

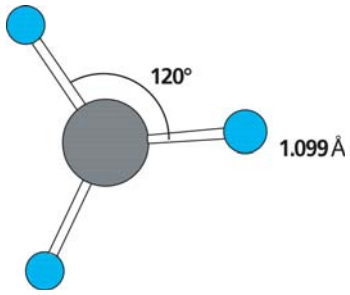

Fig. 4. The optimized geometry of CH_3^+ ion at the MP2/aug-cc-pVDZ level of theory.

with CH_3^- ions in Figure 2 indicates that the primary dissociation process for the CH_3^+ precursor ions involves successive single electron transfers in two collisions, as was observed for other charge inversion processes using alkali metal targets [1,2,6–8,56,59,60].

If the CH_3 radical that is produced from neutralization of CH_3^+ ions is formed in its electronic ground-state, then CH_3^- ions can be formed in a second electron transfer collision because CH_3 has a positive electron affinity of 1.1 eV [61]. Therefore, the absence of CH_3^- ions in the charge inversion spectra also indicates that the neutralization in the single electron transfer for the CH_3^+ precursor ions is near-resonant, and forms the electronically excited CH_3^* radical which dissociates into neutral fragments, as demonstrated for the charge inversion processes using the thermometer molecules on collisions with alkali metal targets [1,5,6].

The peak associated with CH_2^- ions observed at $m/z = 14$ is much more intense than those for the CH^- and C^- ions observed at $m/z = 13$ and 12, respectively, and the shape of the peak associated with the CH_2^- ions observed in the expanded spectrum in Figure 2 resembles a trapezoid. This shape suggests that dissociation is spontaneous from a state with a specific internal energy and without a large energy barrier to dissociation [1,6,62,63].

The heats of formation [61] for the CH_3^+ ion, the CH_3 radical, and those of the fragments formed through dissociation of the CH_3 radical, are shown in Figure 3. From our previous studies using thermometer molecules [1,5,6], it was demonstrated that the neutralization step in the charge inversion process is via near-resonant electron transfer. Supposing that neutralization is resonant, the energy level of the formed neutral species should be lower than the level of the precursor ion by an amount equal to the ionization energy of the target. The energy level associated with a resonance process with the Cs target is shown as dashed line in Figure 3. The energy levels of photo-excitation at 193 nm or 216 nm are also shown in Figure 3. The energy level resulting from near-resonant neutralization is much higher than that of the ground state of the CH_3 radical, as shown in Figure 3. It is possible that this large internal energy could induce the dissociation of the electronically excited CH_3 radical. The dissociations into CH_2 + H and CH + H_2 are energetically possible when the neutralization is near-resonant, and this is believed to be the reason for the absence of CH_3^- ions in the charge inversion spectra.

Typical collision interaction times for the neutralization, where the precursor ions are accelerated by 3.0 kV, is in the range of 10^{-15} s. Since this time is much shorter than the time required for a vibration ($\sim 10^{-13}$ s), the neutralization is expected to be a Franck-Condon process. Therefore, the geometry of the electronically excited CH_3^* radical, which dissociates into fragments, is presumed to be the same as that of the precursor CH_3^+ ion. The optimized geometry of CH_3^+ was calculated at the MP2/ aug-cc-pVDZ level [64], and is shown in Figure 4. The optimized geometry of the CH_3^+ ion has planar D_{3h} symmetry with all C–H bond lengths being equal and the H–C–H bond angle being 120°. Since the neutralization process involves the addition of one electron to the CH_3^+ ion core, the electronically excited CH_3^* radical is presumed to be in the Rydberg state in which one electron is excited. Since the ground electronic state of the CH_3 radical also has D_{3h} symmetry [18], the structure of the transient state formed by photo-absorption has the same D_{3h} symmetry.

As seen in the UV absorption spectra of CH_3 radicals reported by Callear and Metcalfe [11], there are no excitation levels lower than 216 nm (000–000) which corresponds to an energy level 7.25 eV, as shown in Figure 3. The photo-excitation between 204–216 nm was assigned to an electronic transition of the unpaired $2p_z$ electron to a $3s$ Rydberg orbital [11–13,17]. It was also determined that the pre-dissociation of the $3s$ Rydberg state is extremely fast [14,16]. Since the near-resonant level for a Cs target shown as the dashed line in Figure 3 is only 0.19 eV higher than the lowest excited level by photo-absorption, it is proposed that the CH_3^* radicals formed via neutralization in the charge inversion process are in the $3s$ Rydberg state. Orbital correlation reported by Yu et al. [18] show that the $3s$ Rydberg state ($\tilde{B}\ ^2A_1'$) correlates with singlet methylene, CH_2 ($\tilde{a}\ ^1A_1$) with a small barrier (about 0.5 eV) and the ground-state methyl radical correlates to the two asymptotic dissociation channels CH_2 ($\tilde{X}\ ^3B_1$) + H (^2S) and CH ($\tilde{X}\ ^2\Pi$) + H_2 ($^1\Sigma_g^+$).

While the electron affinity of CH_2 ($\tilde{X}\ ^3B_1$) is 0.65 eV, that of CH_2 ($\tilde{a}\ ^1A_1$) was found to be 1.04 eV by using precise photoelectron spectroscopy [65]. Therefore, the CH_2 ($a\ ^1A_1$) radical formed from the dissociation of CH_3^* in the $3s$ Rydberg state can be converted into a negative ion by the second electron transfer collision and detected in the charge inversion mass spectrometry. This feature of the dissociation determined using charge inversion mass spectrometry showed very good agreement with that reported using photoexcitation [11–14,16,17].

The CH^- ion may be produced from the dissociation processes involving both CH + 2H and CH + H_2. The electron affinity of CH ($\tilde{X}\ ^2\Pi$) is 1.28 eV [61], which is larger than that of CH_2($\tilde{a}\ ^1A_1$). Figure 3 shows that two independent C–H bond cleavages are more endothermic than the near-resonant energy levels by 3.26 eV for the Cs target. These large endothermic reactions for CH + 2H should result in a much smaller branching ratio than the exothermic reaction for CH + H_2. Theoretical calculations by Yu et al. [18] indicate that there is a large barrier for the dissociation from the ground CH_3 ($\tilde{X}\ 1\ ^2A_2''$) and also that the excited CH_3 ($\tilde{B}\ 1\ ^2A_1'$) cannot correlatively yield CH ($\tilde{X}^2\Pi$) + H_2($\tilde{X}\ ^1\Sigma_g^+$) by a C_{2v} or C_s-pyramidalized pathway. On the other hand, both more recent investigations via collisions of CH + H_2 [19–22] and theoretical ab initio calculations for the reaction of CH with H_2 [23–25] indicate that reaction of CH + H_2 has little or no activation energy. Lin and coworkers, using laser-induce fluorescence detection of CH radicals in the reaction of CH with H_2 diluted by rare gas at 100 torr total pressure, indicate that the production of CH_3 via collisional stabilization dominated at low temperature (<372 K), while the formation of CH_2 via the decomposition of the excited adduct became more important at high temperature (>372 K) [20]. Liu and coworkers, using a crossed-beam apparatus by the laser-induced fluorescence method, measured the state-to-state integral cross-sections for the isotopic exchange reactions of CH ($X^2\Pi$) and D_2 to give CD ($X^2\Pi$) and its isotopic analog CD ($X^2\Pi$) and H_2 to give CH ($X^2\Pi$) under the collision energy lower than 0.26 eV [21,22]. From the rapid decrease of the cross-section with increasing translational energy, a reaction mechanism based on the formation of a complex was suggested and little or no barrier was estimated for these isotopic exchange reactions [21,22]. The energy region investigated by the reaction of CH and H_2 is lower than the near-resonant level of the CH_3 using the Cs target in the charge inversion process, as shown in Figure 3. Lee and coworkers, using photo-fragment translational spectroscopy, reported [15] that the formation of CH_2 and H(^{2}S) was the only dissociation process on photo-dissociation of CH_3 radicals at 193.3 nm, photoexcitation at 193.3 nm provides a higher energy than that expected from near-resonant neutralization with the Cs target, and those energy levels of the CH_3 radicals are much higher than that of the CH_3 complex investigated via CH + H_2 collisions by Liu and coworkers, as shown in Figure 3.

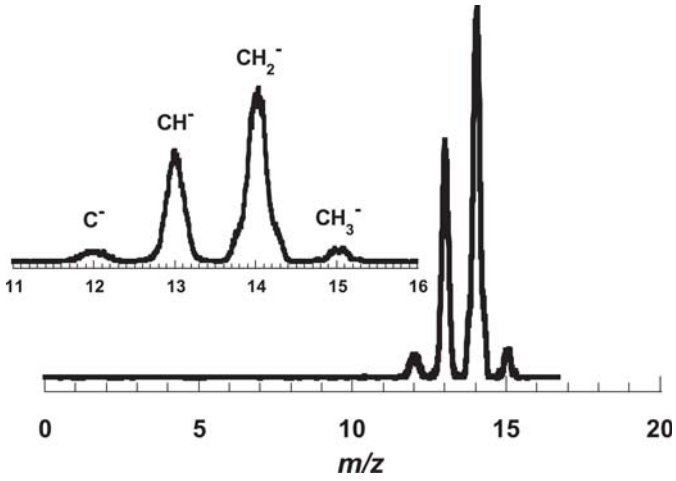

Fig. 5. The charge inversion spectra of CH_4^+ on collision with a Cs target. The expanded spectrum of $m/z = 12{\sim}15$ is shown in the inset.

From the much more abundance of the CH_2^- ion compared with the CH^- ion in the charge inversion spectra shown in Figure 2, it is presumed that the CH_3 radicals in the energy level expected from the near-resonant neutralization dissociate mainly into CH_2 + H rather than into CH + H_2. This presumption apparently contradicts with the recent findings that the reaction of CH + H_2 had little or no activation energy. One plausible explanation that would resolve this apparent contradiction is that the CH_3 radicals in the $3s$ Rydberg state formed via near-resonant neutralization and in the energy state formed by photoabsorption at 193.3 nm dissociate mainly into CH_2 + H, as reported by Weste et al. [14]. and Lee and coworkers [15], while the CH_3 radicals in the state lower than the $3s$ Rydberg state dissociate mainly into CH + H_2 as reported Lin and coworkers [19,20] and Liu and coworkers [21,22] The temperature dependence of the ratio of the CH_2 formation in the reaction between CH + H_2 [19,20] supports this explanation.

3.2 Dissociation of CH_4

The charge inversion spectrum of CH_4^+ ions measured using a Cs target is shown in Figure 5. In this spectrum, the major peak is that associated with CH_2^- ions at $m/z = 14$, whereas the peak associated with CH_3^- ions is much smaller than those of both CH_2^- ions and CH^- ions. The absence of a peak associated with CH_4^- ions is not surprising given that most of the excited CH_4 neutrals formed via neutralization dissociate, and that the electron affinity of CH_4 is negative.

A comparison of the charge inversion spectrum of CH_3^+ ions shown in Figure 2 with that of CH_4^+ ions shown in Figure 5 reveals many differences in intensities and peak shapes. Firstly, while the CH_2^- peak in Figure 2 arising from a single H-atom loss is the dominant peak and has a trapezoidal shape, the equivalent peak in Figure 5, namely the CH_3^- peak, is very small and has a triangular shape.

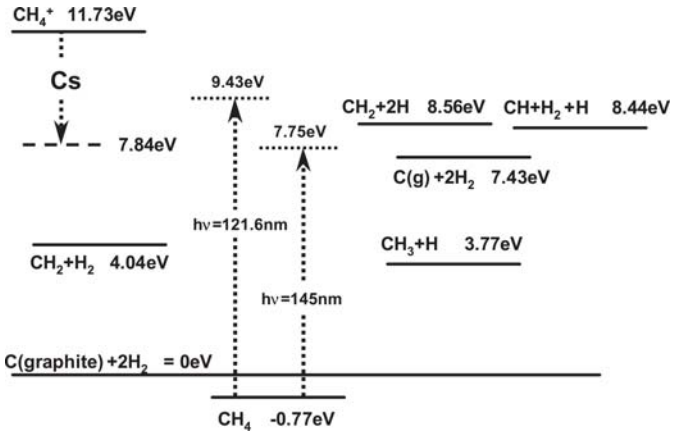

Fig. 6. The heats of formation of the neutral and cationic forms of CH_4. The thermochemical values are taken from reference [61]. The energy levels predicted by near-resonant neutralization with Cs target and photo-excitation are shown as dashed and dotted lines, respectively.

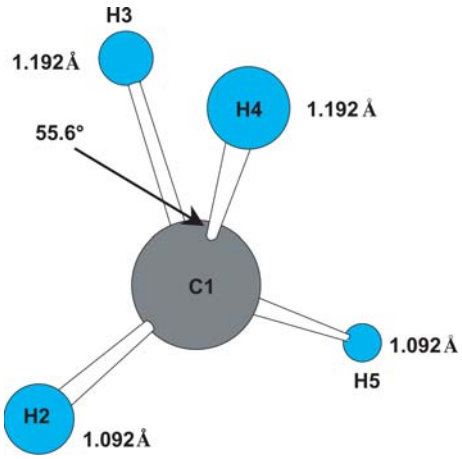

Fig. 7. The optimized geometry of CH_4^+ ion at the MP2/aug-cc-pVDZ level of theory.

In contrast, the CH^- peak in Figure 2 arising from the loss of two H-atoms is much less intense than the CH_2^- peak, whereas the peaks associated with the loss of two or more H-atoms in Figure 5, namely the CH_2^- and the CH^- peak, are both much more intense than the CH_3^- peak.

The electron affinities of C, CH, CH_2, and CH_3 are 1.26 eV, 1.24 eV, 0.65 eV, and 1.1 eV, respectively [61]. Since smaller endothermicities in negative ion formation usually result in larger cross-sections, larger cross-sections are expected for the fragments having higher electron affinities [66]. Since the relative intensities of the individual ion peaks do not depend linearly on electron affinity, the large differences in the peak intensities observed in the charge inversion mass spectra are assumed to be due to the differences in the abundance of the neutral species which results from a difference in the dissociation mechanism between CH_3 and CH_4. As seen in the expanded spectrum in Figure 5, only the peak associated with the CH_2^- negative ion has a shoulder and is thought to consist of two overlapping peaks.

The heats of formation [61] of the CH_4^+ ions, the CH_4 neutral, and those of the fragments formed from the CH_4 neutral are shown in Figure 6, with the energy level associated with the near-resonant neutralization shown as the dashed line. The energy levels of $CH_2 + H_2$ and $CH_3 + H$ are much lower than that of near-resonance shown as the dashed line. The near-resonant level is higher than the energy levels of $C + 2H_2$, and less than 1 eV lower than those of $CH_2 + 2H$ and $CH + H_2 + H$. While the two independent C–H bond cleavages were energetically unfavorable for the CH_3 radical, as shown in Figure 3, two independent C–H bond cleavages in the excited CH_4 neutrals is not so energetically unfavorable, as shown in Figure 6.

Figure 7 shows the optimized geometry of CH_4^+ at the MP2/ aug-cc-pVDZ level of theory [64]. The optimized geometry of CH_4^+ has C_{2v} symmetry. Two of the C–H bonds are significantly stretched compared with the other two, whose lengths are as same as those in the ground state of methane. In the longer C–H bonds, the H3–C1–H4 bond angle is 55.6°, and the H3–H4 distance is 1.11 Å. This small H–H distance is expected to facilitate elimination of an H_2 molecule from the CH_4 neutral, whose geometry is conserved from the CH_4^+ by a Franck-Condon transition. Since the geometry of the CH_4 molecule has T_d symmetry, the excited CH_4^* formed from the CH_4^+ ions of C_{2v} symmetry may provide different dissociation features from those of photo-dissociation.

The start of the absorption spectra of methane at $\lambda = 145.5$ nm indicates that the singlet excited-state of methane exists from 8.52 eV. Theoretical investigations [39–43] indicated that the lowest excited state of methane is the $3s$ Rydberg state which is a degenerate $^1T_2$ formed from $3s \leftarrow 1t_2$ excitation. The vertical excitation energies for $^1T_2$ and $^3T_2$ states were computed to be 10.64–10.66 eV and 10.25–10.30 eV, respectively by Mebel et al. [43], who also reported two minima on the first singlet surface, whose symmetry are C_{3v} and C_{2v} and whose adiabatic excitation energies are 9.16–9.25 eV and 8.39–8.52 eV, respectively. The singlet state with C_{2v} symmetry is estimated to be the lowest state which was observed as absorption from 145.5 nm. It is generally assumed that only the lowest $^1T_2$ state can be accessed at Lyman–α (10.2 eV) photo-absorption. This state of methane is believed to have a short lifetime with respect to dissociation, and correlates adiabatically with the $CH_2(^1B_1) + H_2$ products [39–42]. Mordaunt et al. and Zare and co-workers showed that simple C–H bond fission to form CH_3 fragments was the dominant primary process following excitation by Lyman–α [35,36]. The resulting CH_3 fragments were internally excited and can undergo subsequent decay, predominantly to $CH + H_2$. In contrast to these conclusions favoring the CH_3 fragment in methane photolysis at 10.2 eV, Liu and coworkers reported much larger ratio for the CH_2 fragment from the comparison of the kinetic energy release and anisotropy parameter of the H fragment [37] with CH_2^+ and CH_3^+ ion intensity [38].

In the charge inversion process, both singlet and triplet states of excited neutrals may be formed when the primary positive ion is in a doublet state because the target alkali metal is doublet. In contrast to the case of the CH_3 radical, the symmetry of the positive ion is not same as that of the ground-state neutral. The internal energy of the transient neutral excited by Lyman–α is higher than that expected for the neutral formed via near-resonant neutralization from the positive ion, as shown in Figure 6. Therefore, the dissociation processes of CH_4^* may be different to that of photo-dissociation whose excited state is singlet. However, comparison of the dissociation features in the charge inversion process with photo-dissociation is expected to provide useful insight for the dissociation mechanism of methane.

The heat of formation of the near-resonant level of excited CH_4 formed with a Cs target is 7.84 eV. This energy is only a little higher than the energy level of 7.75 eV that results from photo-absorption at $\lambda = 145.5$ nm. The symmetry of the excited state formed by near-resonant neutralization is presumed to be the same as that of the precursor CH_4^+ ion, namely C_{2v}. Since the symmetry of the excited CH_4 produced by photo-absorption is also reported to be C_{2v} [43], it is expected that near-resonant neutralization occurred using the Cs target.

The singlet $S_1(^1B_1)$ and triplet $T_1(^3B_1)$ of excited CH_4 with C_{2v} symmetry correlated with $CH_2(^1B_1) + H_2$ and $CH_2(^3B_1) + H_2$, respectively, as reported by Mebel et al. [43]. The singlet state comes close to S_0 ($^1A_1$) which correlated with CH_2 ($^1A_1$) + H_2 along the dissociation pathway. The trapezoidal shaped peak associated with the CH_2^- ions in the charge inversion spectrum of CH_4^+ ion can be explained by these dissociation pathways because the trapezoidal shape is indicative of spontaneous dissociation with small activation barrier. This speculation is consistent with earlier experimental and theoretical studies [39–43]. As both singlet and triplet CH_4 can be formed upon neutralization in the charge inversion mass spectrometer, it could not be determined which process was dominant in the dissociation into CH_2+ H_2.

Regarding the excited CH_4 with C_s symmetry, the singlet S_1 ($^1A'$) state and the triplet T_1 ($^3A'$) state correlate with CH_3 ($^2A_1'$) + H and $CH_3(^2A_2'')$ + H, as reported by Mebel et al. [43]. The peak associated with CH_3^- ions in the charge inversion spectrum of CH_4^+ can be explained by these dissociation pathways. We propose that the lower triplet state would be preferential from a thermochemical perspective. When CH_4 dissociates into CH_3 + H, the H-atom has no internal energy, and so the excess energy is divided into kinetic energy of both fragments and internal energy of CH_3. The kinetic energy for this process has been measured in the photo-dissociation of methane at 121.6 nm (10.2 eV) [35,36], whose energy is higher than the near-resonant level, as shown in Figure 6. A very broad kinetic energy distribution was reported, in which extensive fractions of the excess energy was possessed by the CH_3 radical. It was also reported that most of the CH_3 fragments were ro-vibrationally excited, and that they decomposed into CH_2 and CH fragments. The weak intensity of the CH_3^- ion peak compared with the CH_2^- and CH^- ion peaks is explained by this additional dissociation of the excited CH_3.

Dissociation of excited CH_3 has two pathways, namely CH + H_2 and CH_2 + H. Photo-dissociation studies by Mordaunt et al. [35] and Heck et al. [36] do not support the dissociation into CH_2 + H as being the additional dissociation pathway of CH_3 that follows the dissociation of CH_4. It was demonstrated that excited CH_3 with D_{3h} symmetry dissociates predominantly into CH_2 + H, as discussed in the charge inversion spectra of the CH_3^+ ion. While CH_3 with C_{3v} symmetry which is formed from dissociation of CH_4 may correlate with CH + H_2, the energy difference between CH + H_2 and CH_2 + H is very small. The triangular shape peak associated with the CH_2^- ions in Figure 2 clearly indicates the existence of a different pathway for the formation CH_2 apart from CH_2 + H_2. The small kinetic energy estimated from the peak width of the triangular shape supports the existence of an additional dissociation pathway into CH_2 + H.

Liu and coworkers reported that the quantum yields of dissociation pathways in methane photolysis at 10.2 eV are 0.291 ± 0.068 for CH_3 + H, 0.585 ± 0.098 for $CH_2(a\,^1A_1) + H_2$, 0.066 ± 0.012 for $CH_2(a\,^1A_1)$ + 2H, and 0.068 ± 0.013 for CH + H_2 + H [38]. The relative abundance of the CH_2^- ion in the charge inversion mass spectra shown in Figure 5 shows good agreement with the quantum yield of 0.651 ($0.585 + 0.066$) for the CH_2 formation. The existence of two different processes for CH_2 formation in both experiments using the detection of the heavier fragments provided clear evidence that the dissociation of CH_3 with C_{3v} symmetry yields not only CH + H_2 but also CH_2 + H, contrary to the case of the photo-dissociation study detecting only H-atoms and H_2 molecules [35,36]. The relative abundance of the CH_3^- ions shown in Figure 5 is much lower than the quantum yield of 0.291 for the CH_3 formation in the photolysis at 10.2 eV. In contrast to this, the relative abundance of CH^- ions is greater than the quantum yield of 0.068 for the CH formation. These differences between the quantum yield in the photolysis and the relative intensities in the charge inversion spectra may be attributed to the differences for the negative ion formation cross-sections depending on the neutral species in the charge inversion spectra. Another reason to be considered is the difference of internal energies of CH_4^* between the both experiments. The near-resonant level using the Cs target is lower by 1.59 eV than the energy level obtained by Lyman–α photo-absorption, as shown in Figure 6, and is lower than that of CH + H_2+ H. Therefore, the large CH^- ion intensity cannot be explained by the near-resonant neutralization, as shown in Figure 6. While the reason for this apparently anomalous results is not understood at present, we suspect there are two possible reasons for the higher internal energy of CH_4^* neutrals formed in the charge inversion mass spectrometry, namely; (i) the electronic or vibrational excitation of the precursor CH_4^+ ions which form in the ion source, or (ii) the internal energy of CH_4^* which was converted from the collision energy of the CH_4^+ ions in the keV energy collision.

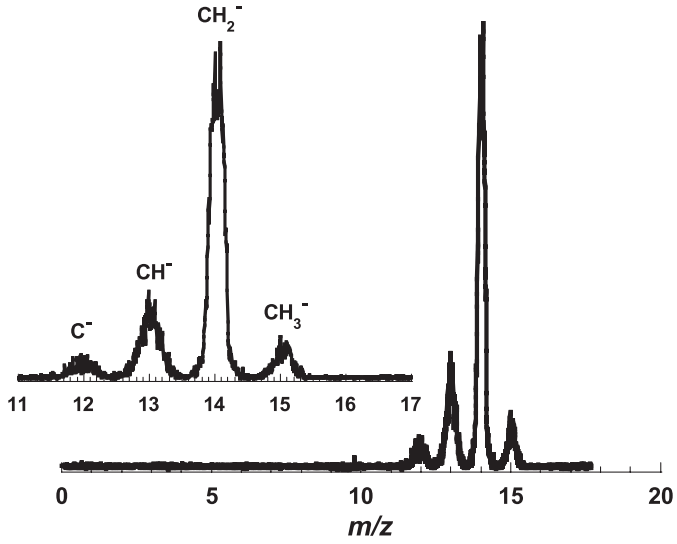

Fig. 8. The charge inversion spectra of CH_5^+ on collision with a Cs target. The expanded spectrum of $m/z = 12{\sim}15$ is shown in the inset.

3.3 Dissociation of CH_5

Figure 8 shows the charge inversion mass spectrum of CH_5^+ ions measured under chemical ionization (CI) conditions since precursor CH_5^+ ions cannot be produced under electron ionization (EI) conditions. In the charge inversion spectra of CH_5^+ ions, the peak at $m/z = 14$ associated with CH_2^- ions is dominant, and the peaks associated with C^- and CH_3^- ions are less intense than that for CH^- ions. At first glance, the charge inversion spectrum of CH_5^+ ion appears similar to that of CH_4^+ ions shown in Figure 5. Since the abundance of CH_5^+ ions was much greater than that of CH_4^+ ions in the CI mass spectrum, the influence of $^{13}CH_4^+$ is expected to be very small. If $^{13}CH_4^+$ ions were dominant in the precursor ions having $m/z = 17$, the m/z values of the respective peaks in the charge inversion spectra would have been shifted 1 u towards higher m/z value. Therefore, the affect of any $^{13}CH_4^+$ ions in this experiment is negligible. The absence of a peak at $m/z = 16$ in the charge inversion spectrum, which would have resulted upon H-atom loss from the transient CH_5 neutral, is consistent with the negative electron affinity of methane.

The heats of formation [61] of the CH_5^+ ions, and those of the fragments formed from the CH_5 radical are shown in Figure 9. The energy level associated with the near-resonance neutralization is shown as dashed line in Figure 9. In contrast to the case of CH_3 and CH_4, there have been no reports on photo-excitation of CH_5, so the energy levels associated with photo-excitation are not included in this diagram. The energy level associated with the near-resonant level achieved using a Cs target is much higher than those of $CH_3 + H_2$ and $CH_4 + H$. The relationship between the exothermicity and the energy levels of the fragments shown in Figure 9 is not the same as for CH_3 shown in Figure 3 but is the same as the case of CH_4 shown in Figure 6.

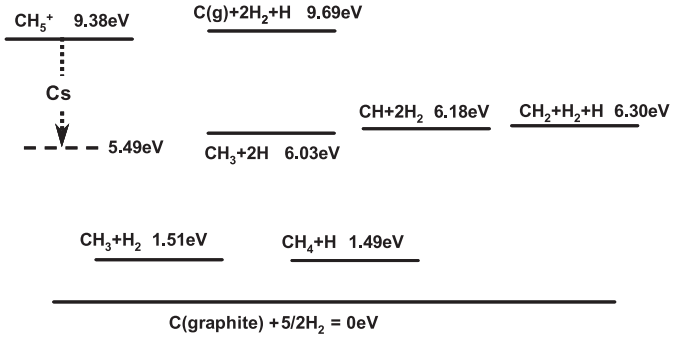

Fig. 9. The heats of formation of the neutral and cationic forms of CH_5. The thermochemical values are taken from reference [61]. The energy levels predicted by near-resonant neutralization is shown as a dashed line.

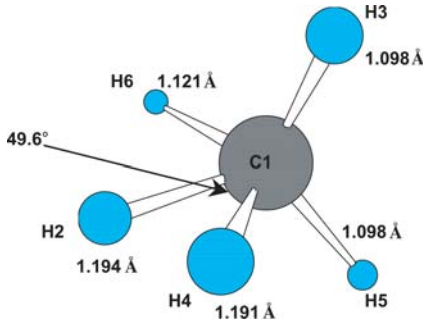

Fig. 10. The optimized geometry of CH_5^+ ion at the MP2/aug-cc-pVDZ level of theory.

Figure 10 shows the optimized geometry of CH_5^+ calculated at the MP2/aug-cc-pVDZ level of theory [64]. The optimized geometry of CH_5^+ has C_s symmetry, which is in agreement with earlier theoretical calculations [47–54]. Two of the C–H bonds are significantly longer than those of other three C–H bonds. In the longer C–H bonds, the H2–C1–H4 bond angle is 49.6°, and the H2–H4 distance is 1.00 Å.

The primary differences between the charge inversion spectra of CH_4^+ ions (Fig. 5) and CH_5^+ ions (Fig. 8) are the peak shapes of the CH_2^- ions and intensities of the CH_2^- peaks relative to the CH^- peaks. The triangular shape of the peak associated with the CH_2^- ions (in Fig. 8) indicates that the CH_2 fragments are not formed solely through direct dissociation with very small energy barrier. It is reasonable to assume that direct H_3 loss from the excited CH_5 neutral is unlikely, but that simultaneous loss of an H_2 molecule and an H-atom may be involved. Since CH_5^+ ions are formed under CI conditions, the precursor CH_5^+ ions in the charge inversion process are expected to be in their electronic ground-state. The binding energy between CH_3^+ and H_2 in the CH_5^+ ions is estimated to be in the range 40–45 kcal/mole (1.73–1.95 eV) according both to thermochemical and theoretical data [54, 61]. When CH_5^+ ions having the structure shown in Figure 10 are neutralized, it is expected that the weakest bond is cleaved and produces $CH_3 + H_2$. This dissociation mechanism is consistent with the relatively intense peak

associated with CH_3^- ion observed in Figure 8 because CH_3 has a positive electron affinity of 1.1 eV. Nevertheless, as seen in Figure 8, the intensity of the CH_3^- ion peak is still much smaller than that of the CH_2^- ion. The lower abundance of CH_3^- ions compared with CH_2^- ions can be explained by the additional dissociation that is likely to occur in the CH_3 fragment due to its highly deformed structure relative to the calculated equilibrium structure, as was the case for CH_4.

In the equilibrium geometry of CH_4^+, which has C_{2v} symmetry, the H–C–H bond angles of the CH_3 fragment are H5–C1–H4 = 114.0°, H2–C1–H5 = 125.4°, H4–C1–H2 = 113.9°, respectively, while in the case of CH_5^+, which has C_s symmetry, the bond angles are H3–C1–H5 = 120.2°, H6–C1–H3 = 108.4°, H5–C1–H6 = 108.3°, respectively. If the CH_3 fragments formed by H-atom loss and H_2 molecule loss from CH_4 and CH_5 neutrals, respectively, have planer D_{3h} symmetry, then the sum of the three H–C–H bond angles should be 360°. In the case of CH_4^+ and CH_5^+, the sum of the three H–C–H bond angles are 353.3° and 336.9°, respectively. Judging from these values, CH_3 fragments formed through loss of H_2 from CH_5 neutrals may be highly deformed compared with CH_3 fragments formed through H-atom loss from CH_4 neutrals. As discussed above for CH_4, the more deformed structure in the CH_3 having C_{3v} symmetry is expected to facilitate dissociation into CH + H_2 rather than that into CH_2 + H. However, the larger intensity of the CH^- ion peak relative to the CH_2^- ion peak in the charge inversion spectra of CH_4^+ ions shown in Figure 5, compared with CH_5^+ ions in Figure 8 contradict this expectation. One plausible explanation that would resolve this apparent contradiction, is that dissociation of CH_4 neutrals resulting from dissociation of CH_5 into CH_4 + H might contribute to the formation of extra CH_2 fragments through dissociation into CH_2 + H_2.

Although some unresolved questions remain about the dissociation of electronically excited CH_5, the main features of the dissociation of excited CH_5 have been revealed through the use of charge inversion mass spectrometry of protonated methane. Comparison with theoretical results will provide new information about the dissociation dynamics of reaction intermediates, such as CH_5, because the CH_5 neutral is assumed to have structure resembling an intermediate in association reaction of CH_3 + H_2 or CH_4 + H.

4 Conclusion

In the charge inversion spectrum of CH_3^+ ions, the peak associated with CH_2^- ions is the most intense and has a trapezoidal shape. The process leading to the formation of CH_2^- ions is attributed to the spontaneous dissociation of the 3*s* Rydberg state of CH_3 radicals, formed via near-resonant neutralization, into CH_2 + H. The much less abundance of the CH^- ion compared with the CH_2^- ion is considered to be the result of the small branching ratio in dissociation of the CH_3 radicals in the 3*s* Rydberg state into CH + H_2, since it is indicated that the dissociation process into CH + H_2 of the CH_3 radical in lower energy states than the 3*s* Rydberg state has no activation barrier [21,22].

In the charge inversion spectrum of CH_4^+ ions, the peak associated with CH_2^- ions is, again, the most intense and comprised a combined trapezoidal-shaped peak and triangular-shape peak. The trapezoidal-shaped peak is attributed to direct dissociation of excited CH_4 into CH_2 + H_2, where the CH_4 have the same C_{2v} symmetry as that of the ground-state CH_4^+ cation. Although the peak associated with H-atom loss is much more intense than that associated with H_2 loss in the charge inversion spectrum of the CH_3^+ ions, in the case of the charge inversion spectrum of CH_4^+, the CH_3^- ion peak associated H-atom loss is much less intense than the CH_2^- ion peak. This difference between the charge inversion spectra of CH_3^+ and CH_4^+ is explained on the basis that the CH_3 formed from the dissociation of CH_4 into CH_3 + H has a shape that is deformed from D_{3h} symmetry and so undergoes further subsequent dissociation into CH_2 + H or CH + H_2. This explanation is consistent with the dissociation processes of the CH_4 molecule in the 3*s* Rydberg state formed by Lyman–α photo-excitation. This additional dissociation of the deformed CH_3 into CH_2 + H is proposed to result in the triangular-shaped portion of the CH_2^- peak. Furthermore, the additional dissociation of the deformed CH_3 into CH + H_2 is proposed as the reason for the peak associated with CH^- ions being more intense than that associated with CH_3^- ions.

The use of charge inversion mass spectrometry has enabled the dissociation process of the CH_5 neutral, which is formed via near-resonant neutralization of the CH_5^+ ion, to be investigated for the first time. In the charge inversion spectrum of the CH_5^+ ion, the peak associated with CH_2^- ions was much more intense than those associated with CH^- ions and CH_3^- ions. Although CH_4 may be formed as a result of dissociation of the CH_5 radical into CH_4 + H, the absence of a CH_4^- ion peak in the charge inversion spectrum of CH_5^+, is attributed to the negative electron affinity of the CH_4 molecule. The fact that the peak associated with the CH_3^- ion was much weaker than that of the CH_2^- ion indicates that the shape of the CH_3 fragment formed on dissociation of CH_5 into CH_3 + H_2 is highly distorted from D_{3h} symmetry, as was the case for CH_4, and its formation is followed by subsequent dissociation. This speculation that the CH_3 radical formed from CH_5 is deformed is supported by the CH_5^+ structure calculated by ab initio calculation.

The approach employed in this work involving the detection and analysis of heavier fragments of electronically excited neutrals formed from the corresponding cations has provided useful complementary information to that previously available from photo-dissociation measurements. This investigation has demonstrated that the charge inversion method using an alkali metal target can easily provide useful information about the dissociation of unusual radicals such as CH_3 and CH_5. We have demonstrated that neutrals corresponding to protonated

molecules, which are assumed to have structures resembling reaction intermediates, can now be accessed through neutralization in an isolated system, and it is, therefore, expected that these unusual neutrals will be investigated widely using charge inversion mass spectrometry.

Grant-in-Aid for scientific research from the Ministry of Education, Culture, Sports, Science and Technology under Grant No. 13640515 is gratefully acknowledged. We also gratefully acknowledge the support of Library & Science Information Center, Osaka Prefecture University.

References

1. S. Hayakawa, Int. J. Mass Spectrom. **212**, 229 (2001)
2. S. Hayakawa, J. Mass Spectrom. **39**, 111 (2004)
3. V.H. Wysocki, H.I. Kenttamaa, R.G. Cooks, Int. J. Mass Spectrom. Ion Processes **75**, 181 (1987)
4. L.E. Dejarme, R.G. Cooks, T. Ast, Org. Mass Spectrom. **27**, 667 (1992)
5. S. Hayakawa, K. Harada, K. Arakawa, N. Morishita, J. Chem. Phys. **112**, 8432 (2000)
6. S. Hayakawa, K. Harada, N. Watanabe, K. Arakawa, N. Morishita, Int. J. Mass Spectrom. **202**, A1 (2000)
7. S. Hayakawa, M. Takahashi, K. Arakawa, N. Morishita, J. Chem. Phys. **110**, 2745 (1999)
8. S. Hayakawa, K. Tomozawa, T. Takeuchi, N. Morishita, Phys. Chem. Chem. Phys. **5**, 2386 (2003)
9. G. Herzberg, J. Shoosmith, Can. J. Phys. **34**, 523 (1956)
10. G. Herzberg, Proc. R. Soc. Lond. A **262**, 291 (1961)
11. A.B. Callear, M.P. Metcalfe, Chem. Phys. **14**, 275 (1976)
12. J. Danon, H. Zacharias, H. Rottke, H.H. Welge, J. Chem. Phys. **76**, 2399 (1982)
13. T.G. DiGiuseppe, J.W. Hudgens, M.C. Lin, J. Phys. Chem. **86**, 36 (1982)
14. S.G. Westre, P.B. Kelly, Y.P. Zhang, L.D. Ziegler, J. Chem. Phys. **94**, 270 (1991)
15. S.W. North, D.A. Blank, P.M. Chu, Y.T. Lee, J. Chem. Phys. **102**, 792 (1995)
16. T.B. Settersten, R.L. Farrow, J.A. Gray, Chem. Phys. Lett. **370**, 204 (2003)
17. G. Wu, B. Jiang, Q. Ran, J. Zhang, S.A. Harich, X. Yang, J. Chem. Phys. **120**, 2193 (2004)
18. H.T. Yu, A. Sevin, E. Kassab, E.M. Evleth, J. Chem. Phys. **80**, 2049 (1984)
19. M.R. Berman, M.C. Lin, J. Chem. Phys. **81**, 5743 (1984)
20. S. Zabarnick, J.W. Fleming, M.C. Lin, J. Chem. Phys. **85**, 4373 (1986)
21. K. Liu, R.G. Macdonald, J. Chem. Phys. **89**, 4443 (1988)
22. R.G. Macdonald, K. Liu, J. Chem. Phys. **93**, 2443 (1990)
23. B.R. Brooks, H.F. Schaefer III, J. Chem. Phys. **67**, 5146 (1977)
24. T.H. Dunning, Jr, L.B. Harding, R.A. Bair, R.A. Eades, R.L. Shepard, J. Phys. Chem. **90**, 344 (1986)
25. M. Duran, Y. Yamaguchi, H.F. Schaefer III, J. Phys. Chem. **92**, 3070 (1988)
26. J.S. Levine, *The photochemistry of atmosphere* (Academic, New York, 1985)
27. R.P. Wayne, *Chemistry of Atmosphere* (Oxford University, New York, 1991)
28. L.M. Lara, R.D. Lorents, R. Rodrigo, Planet. Space Sci. **42**, 5 (1994)
29. G. Herzberg, *Molecular spectra and Molecular structure III, electronic spectra and electronic structure of Polyatomic molecules* (van Nostrand Reihold, New York, 1966)
30. Okabe, *Photochemistry of Small Molecules* (Willey, New York, 1978)
31. L.C. Lee, C.C. Chiang, J. Chem. Phys. **78**, 688 (1983)
32. G. Ma, M. Suto, L.C. Lee, J. Quant. Radiant. Transfer. **44**, 379 (1990)
33. M.G. Curtis, I.C. Walker, J. Chem. Soc. Faraday Trans. **85**, 659 (1989)
34. T.M. Slanger, G. Black, J. Chem. Phys. **77**, 2432 (1982)
35. D.H. Mordaunt, I.R. Lambert, G.P. Morley, M.N.R. Ashfold, R.N. Dixon, C.M. Western, L. Schnieder, K.H. Welge, J. Chem. Phys. **98**, 2054 (1993)
36. A.J.R. Heck, R.N. Zare, D.W. Chandler, J. Chem. Phys. **104**, 4019 (1996)
37. J.-H.Wang, K. Liu, J. Chem. Phys. **109**, 7105 (1998)
38. J.-H. Wang, K. Liu, Z. Min, H. Su, R. Bersohn, J. Preses, J.Z. Larese, J. Chem. Phys. **113**, 4146 (2000)
39. S. Karplus, R. Bersohn, J. Chem. Phys. **51**, 2040 (1969)
40. M.S. Gordon, Chem. Phys. Lett. **52**, 161 (1977)
41. M.S. Gordon, J.W. Caldwell, J. Chem. Phys. **70**, 5503 (1979)
42. H.U. Lee, R. Janoschek, Chem. Phys. **39**, 271 (1979)
43. A.M. Mebel, S.H. Lin, C.H. Chang, J. Chem. Phys. **106**, 2612 (1997)
44. D.P. Stevenson, D.O. Schissler, J. Chem. Phys. **23**, 1353 (1955)
45. D.O. Schissler, D.P. Stevenson, J. Chem. Phys. **24**, 926 (1956)
46. V.L. Talroze, A.L. Lyubimova, Doll. Akad. Nauk SSSR **86**, 509 (1952)
47. W.A. Lathan, W.J. Hehre, J.A. Pople, J. Am. Chem. Soc. **93**, 808 (1971)
48. V. Dyczmons, W. Kutzelnigg, Theor. Chim. Acta **33**, 239 (1974)
49. K. Raghavachari, R.A. Whiteside, J.A. Pople, P.v.R. Schleyer, J. Am. Chem. Soc. **103**, 5649 (1981)
50. K. Hirao, S. Yamabe, Chem. Phys. **89**, 237 (1984)
51. A. Komornicki, D.A. Dixon, J. Chem. Phys. **86**, 5625 (1987)
52. P.R. Schreiner, S.-J. Kim, H.F. Schaefer III, P.v.R. Schleyer, J. Chem. Phys. **99**, 3716 (1993)
53. M. Kolbuszewski, P.R. Bunker, J. Chem. Phys. **105**, 3649 (1996)
54. P.v.R. Schleyer, J.W. de M. Carneiro, J. Comput. Chem. **13**, 997 (1992)
55. K. Hiraoka, I. Kudaka, S. Yamabe, Chem. Phys. Lett. **184**, 271 (1991)
56. S. Hayakawa, H. Endoh, K. Arakawa, N. Morishita, T. Sugiura, Int. J. Mass Spectrom. Ion Processes **151**, 89 (1995)
57. S. Hayakawa, N. Terazawa, T. Sugiura, J. Phys. B **23**, 4539 (1990)
58. S. Hayakawa, N. Terazawa, T. Sugiura, J. Mass Spectrom. Soc. Jpn **41**, 225 (1993)
59. S. Hayakawa, H. Endoh, K. Arakawa, N. Morishita, Int. J. Mass Spectrom. Ion Processes **171**, 209 (1997)
60. S. Hayakawa, K. Kadomura, M. Kimura, C.M. Dutta, Phys. Rev. A **70**, 022708-1 (2004)

61. S.G. Lias, J.E. Liebman, J.H. Holmes, R.D. Levin, W.G. Mallard, J. Phys. Chem. Ref. Data **17**, (Suppl 1) (1988)
62. S. Hayakawa, M. Yoshioka, T. Sugiura, Int. J. Mass Spectrom. Ion Processes **87**, 309 (1989)
63. S. Hayakawa, M. Mori, N. Watanabe, K. Fujii, K. Arakawa, N. Morishita, J. Mass Spectrom. Soc. Jpn **49**, 144 (2000) (in Japanese)
64. *Gaussian 03, Revision B.05*, M.J. Frisch, G.W. Trucks, H.B. Schlegel, G.E. Scuseria, M.A. Robb, J.R. Cheeseman, J.A. Montgomery Jr, T. Vreven, K.N. Kudin, J.C. Burant, J.M. Millam, S.S. Iyengar, J. Tomasi, V. Barone, B. Mennucci, M. Cossi, G. Scalmani, N. Rega, G.A. Petersson, H. Nakatsuji, M. Hada, M. Ehara, K. Toyota, R. Fukuda, J. Hasegawa, M. Ishida, T. Nakajima, Y. Honda, O. Kitao, H. Nakai, M. Klene, X. Li, J.E. Knox, H.P. Hratchian, J.B. Cross, C. Adamo, J. Jaramillo, R. Gomperts, R.E. Stratmann, O. Yazyev, A.J. Austin, R. Cammi, C. Pomelli, J.W. Ochterski, P.Y. Ayala, K. Morokuma, G.A. Voth, P. Salvador, J.J. Dannenberg, V.G. Zakrzewski, S. Dapprich, A.D. Daniels, M.C. Strain, O. Farkas, D.K. Malick, A.D. Rabuck, K. Raghavachari, J.B. Foresman, J.V. Ortiz, Q. Cui, A.G. Baboul, S. Clifford, J. Cioslowski, B.B. Stefanov, G. Liu, A. Liashenko, P. Piskorz, I. Komaromi, R.L. Martin, D.J. Fox, T. Keith, M.A. Al-Laham, C.Y. Peng, A. Nanayakkara, M. Challacombe, P.M.W. Gill, B. Johnson, W. Chen, M.W. Wong, C. Gonzalez, J.A. Pople, Gaussian Inc., Pittsburgh PA, 2003
65. D.G. Leopold, K.K. Murray, Amy E.S. Miller, W.C. Lineberger, J. Chem. Phys. **83**, 4849 (1985)
66. D. Rapp, W.E. Francis, J. Chem. Phys. **37**, 2631 (1962)